Improvements to a physiological model used for hearing aid evaluation and design

M. S. Arefeen Zilany (zilany@grads.ece.mcmaster.ca) and **Ian C. Bruce**
Department of Electrical and Computer Engineering, McMaster University, Hamilton, Ontario, Canada

McMaster University

AUDITORY ENGINEERING LABORATORY

1. Introduction

Computational models have been developed by Carney and colleagues to simulate the responses of auditory nerve (AN) fibers in cat (Carney, JASA 1993; Zhang et al., JASA 2001; Tan and Carney, JASA 2003). The most recent version adds a level-independent instantaneous frequency glide in the basilar membrane (BM) filter, as observed in BM and AN data. This model produces realistic responses to simple acoustic stimuli but has not applied to the study of AN responses to speech. The Zhang et al. (2001) version of the model has been modified by Bruce and colleagues (JASA 2003) to study the effects of outer and inner hair cell impairment on the AN's representation of speech stimuli. However, the Bruce et al. model did not address the instantaneous frequency glides in the impulse response of AN fibers, which may explain the shifts in best frequency (BF) following impairment of outer hair cells or at high intensities in the normal cochlea. In this paper, an improved model has been developed by substituting the BM gammatone filter of the Bruce et al. model by a chirp filter from the recent version of the model by Tan and Carney (2003). The motivation for the development of this model is to provide a more accurate description of the responses of AN fibers to speech sounds to be useful in testing the effects of potential hearing-aid speech processing schemes.

2. The Model

The model of Bruce and colleagues is an extended version of the previous model developed by Zhang et al. (2001), which included compression, suppression and level-dependent bandwidths and phases. In the Bruce et al. model, the wide-band feedforward control path was modified and a middle ear filter was added, both of which helped improve the model's response to wide-band stimuli such as speech signals. However, replacing the BM filter of the Bruce et al. model by a chirp filter that produces frequency glides in the impulse response of AN fibers should enhance the ability of the model to predict AN responses to speech stimuli.

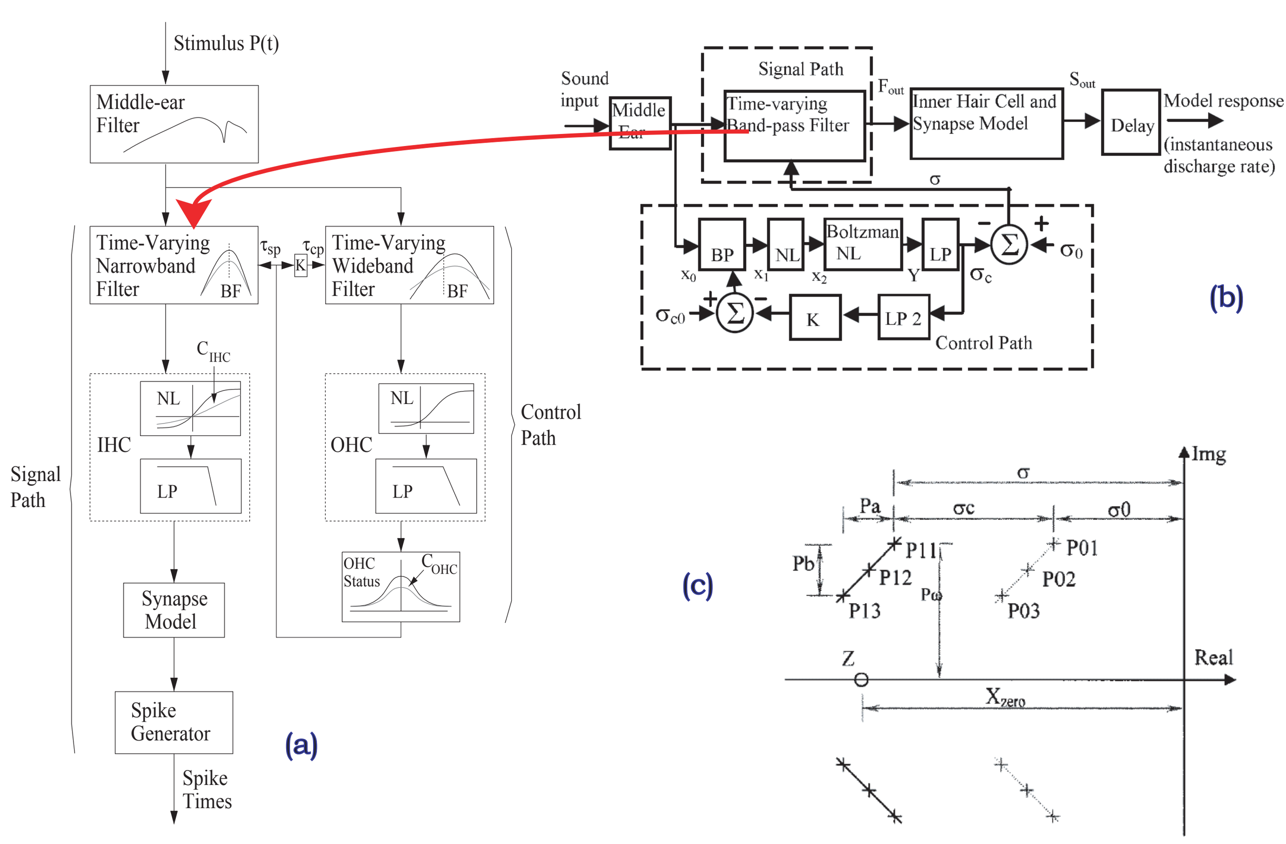

Fig. 1. (a) The auditory-periphery model modified from Zhang et al. (2001) by Bruce et al. (2003). (b) Schematic diagram of the AN model by Tan and Carney (2003). Abbreviation: outer hair cell (OHC), inner hair cell (IHC), low-pass filter (LF), static nonlinearity (NL), best frequency (BF), band-pass filter (BP). (c) Pole-zero locations for the bandpass filter in the model's signal path. σ_0 is the real part of the pole when the siganl intensity is zero, and σ_c is the control signal.

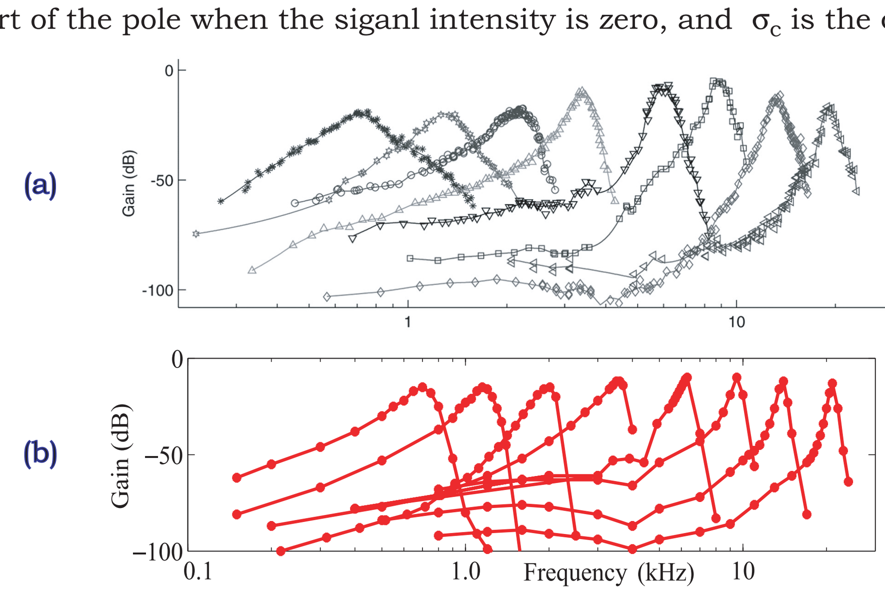

Fig. 2. Amplitude curves from AN of a cat. BFs range from 740 Hz to 19.7 kHz. Individual curves have been vertically offset according to the respective thresholds of the fiber. (a) Redrawn from Heijden et al. (2003). (b) Results from new model.

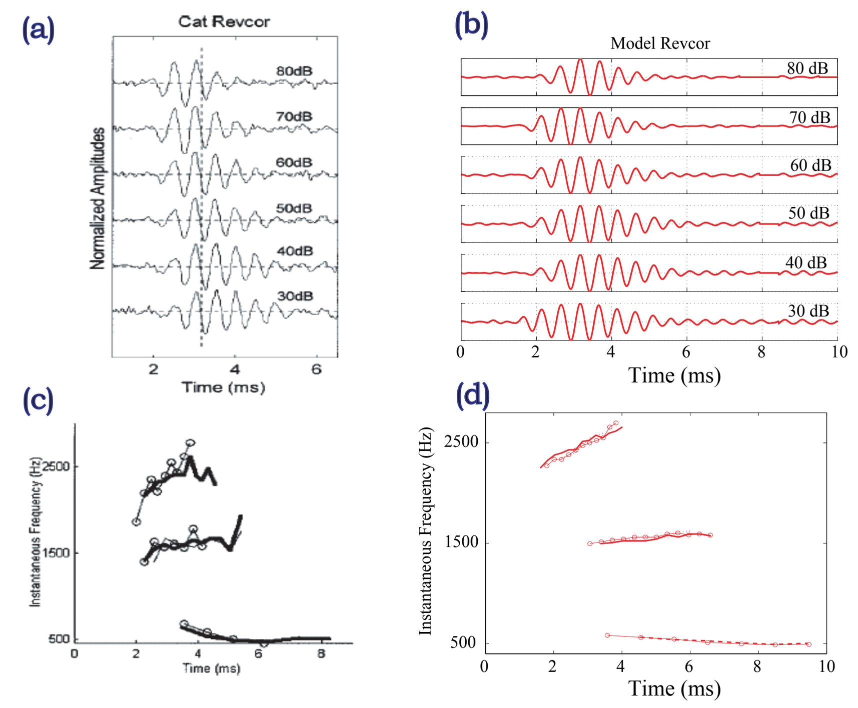

Fig. 3. Revcor functions and instantaneous frequency profiles (a)Measured revcor functions for AN fiber with BF = 2060 Hz at six levels: 30 to 80 dB SPL (unit 86100-25 from Carney and Yin,1988) (b) Model revcor functions for a fiber with matching BF. All revcor functions are normalized to their peak amplitude. (c) Measured AN instantaneous frequency glides calculated based on zero-crossings from revcor functions with 40, 60 and 80 dB for BFs 550, 1600 and 2500 Hz. (d) Model AN instantaneous frequency profiles for fibers with BFs matching the measured fibers. It shows that instantaneous-frequency glides are almost level- independent.

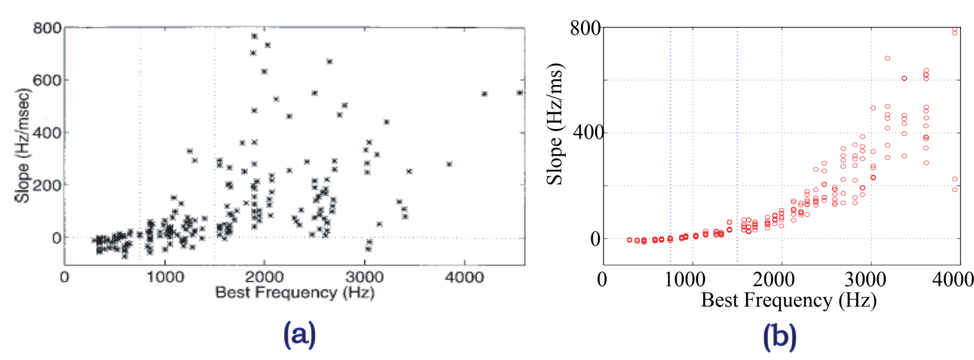

Fig. 4. Slope of the 1st-order regressions of IF trajectories based on responses at several SPLs on a linear frequency axis. The BF for each fiber is determined by averaging the BFs across the SPLs studied. (a) Measured for 214 fibers in 13 cats (Carney et al. 1999). (b) Model IF trajectories for several BFs at 40 to 100 dB SPLs. Vertical dotted lines are positioned at 750 and 1500 Hz to distinguish among the downward, constant and upward frequency glides.

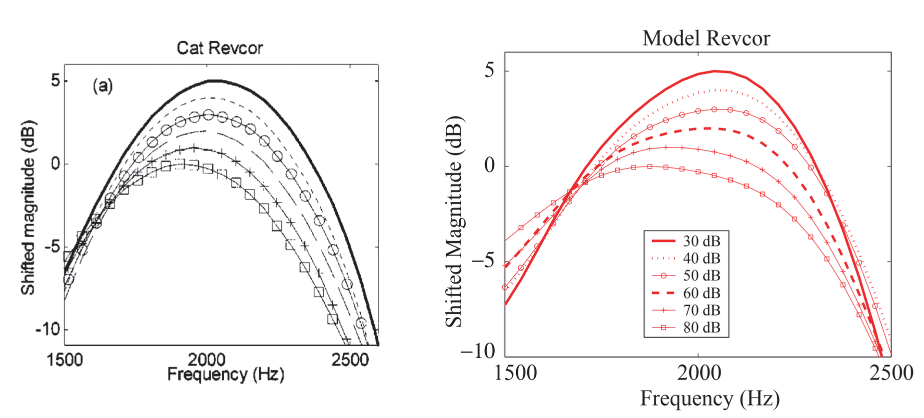

Fig. 5. Measured and model reverse-correlation filters. The magnitudes of the revcor filters were computed for wideband noise presented at stimulus levels from 30 to 80 dB SPL. Each revcor filter is normalized by its peak value; for clarity, a 1-dB shift is introduced between filters computed at different noise levels. The measured responses are from unit 86100-25 from Carney and Yin (1988).

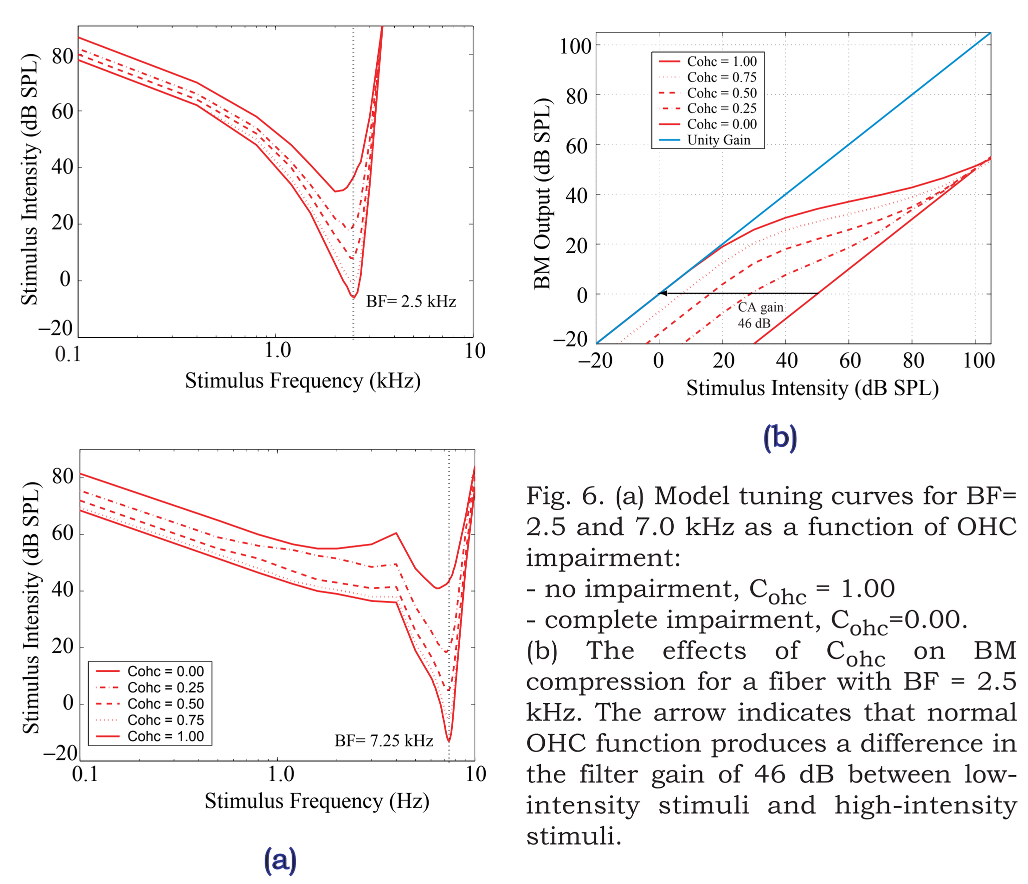

Fig. 6. (a) Model tuning curves for BF= 2.5 and 7.0 kHz as a function of OHC impairment:
- no impairment, $C_{ohc} = 1.00$
- complete impairment, C_{ohc}=0.00.

(b) The effects of C_{ohc} on BM compression for a fiber with BF = 2.5 kHz. The arrow indicates that normal OHC function produces a difference in the filter gain of 46 dB between low-intensity stimuli and high-intensity stimuli.

3. Results

The basic response properties of the model are quite satisfactory, as seen in the figures.

Predictions shown in figure 7 have been obtained for model fibers with BFs roughly covering the range of BFs in the Wong et al. (1998) data. Consistent with the physiological data, the new model predictions for normal OHC and IHC function exhibit synchrony capture by F2 at moderate levels. Also seen in the model predictions is the transition in synchrony from F2 to F1 at higher intensities and the stimulus intensity at which the switch occurs is decreasing with incresing BF. The new model better predicts this switch in synchrony capture than the Bruce et al. model.

In figure 8, the model predictions for normal fibers are predominantly within the range of values seen in the physiological data. Normal fibers synchronize almost exclusively to the formant frequency closest to their BFs. The small peak in F1 PR of the model predictions at 1 kHz is due to the harmonic distortion in the nonlinear BM filter. With impaired OHC and IHC function, model predictions of PRs fall within the range of single-fiber values for F1 and F3, but not for F2. Synchrony to F2 is overestimated in the BF region around F2. An upward shift in the peaks of F1 and F2 synchrony is observed in the model

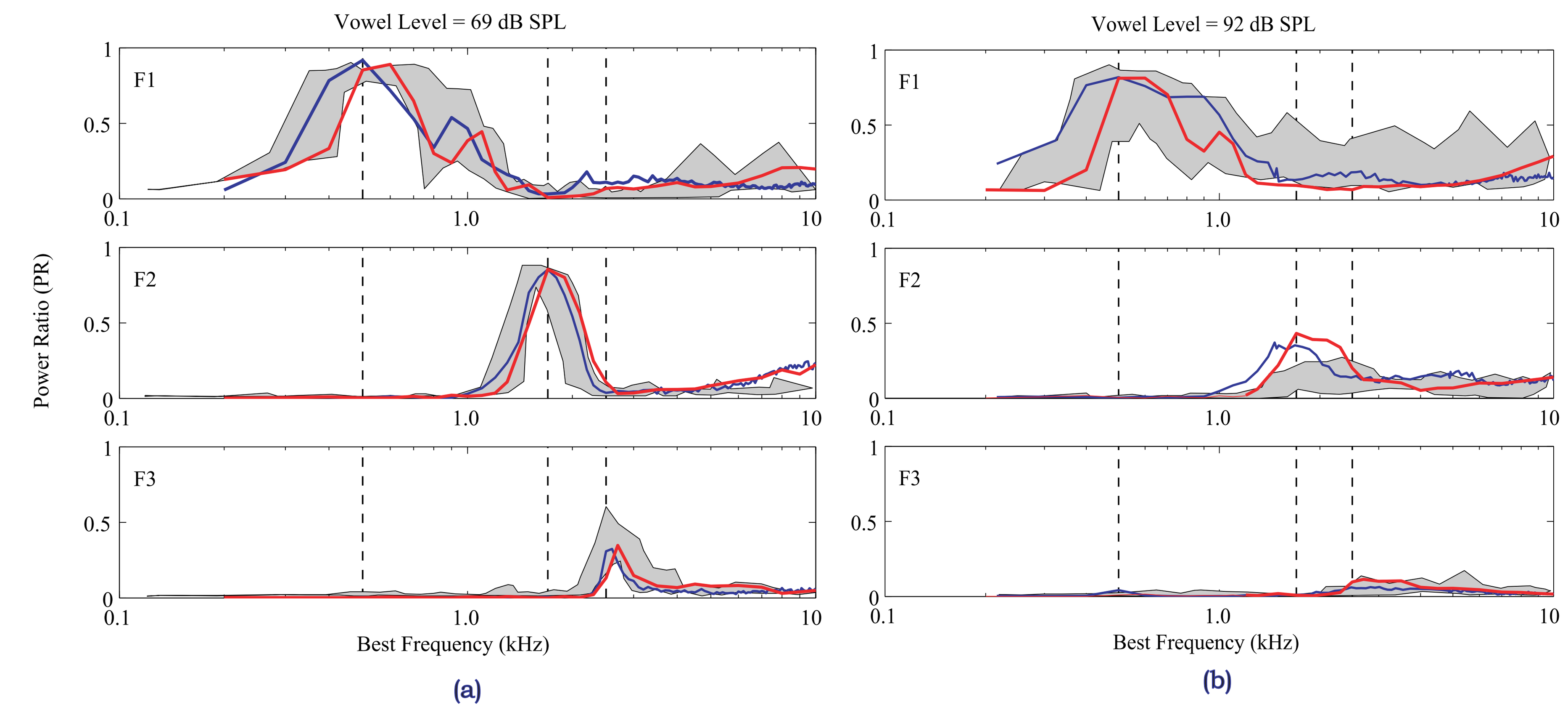

Fig. 8. (a) Model predictions of normal power ratios for F1, F2 and F3 as a function of normal BF for stimulus intensities of 69 dB SPL. (b) Model predictions of impaired power ratios for the 3 formants as a function of impaired BF for stimulus intensities of 92 dB SPL. Thick lines show model predictions (**Blue: Bruce et al. Model** 2003, **Red: New Model**) and gray hatched area indicate the range of values observed in normal (a) and impaired (b) physiological data of Miller et al. (1997). Vertical dashed lines show the formant frequencies. Predictions are shown for model Q_{10} values that are 50^{th} percentile of the Q_{10} values for the normal (a) and impaired (b) physiological data. PRs here include the phase-locked response to the first, second and third harmonics of the formant frequency, as long as the frequency of the harmonic is less than or equal to 5 kHz.

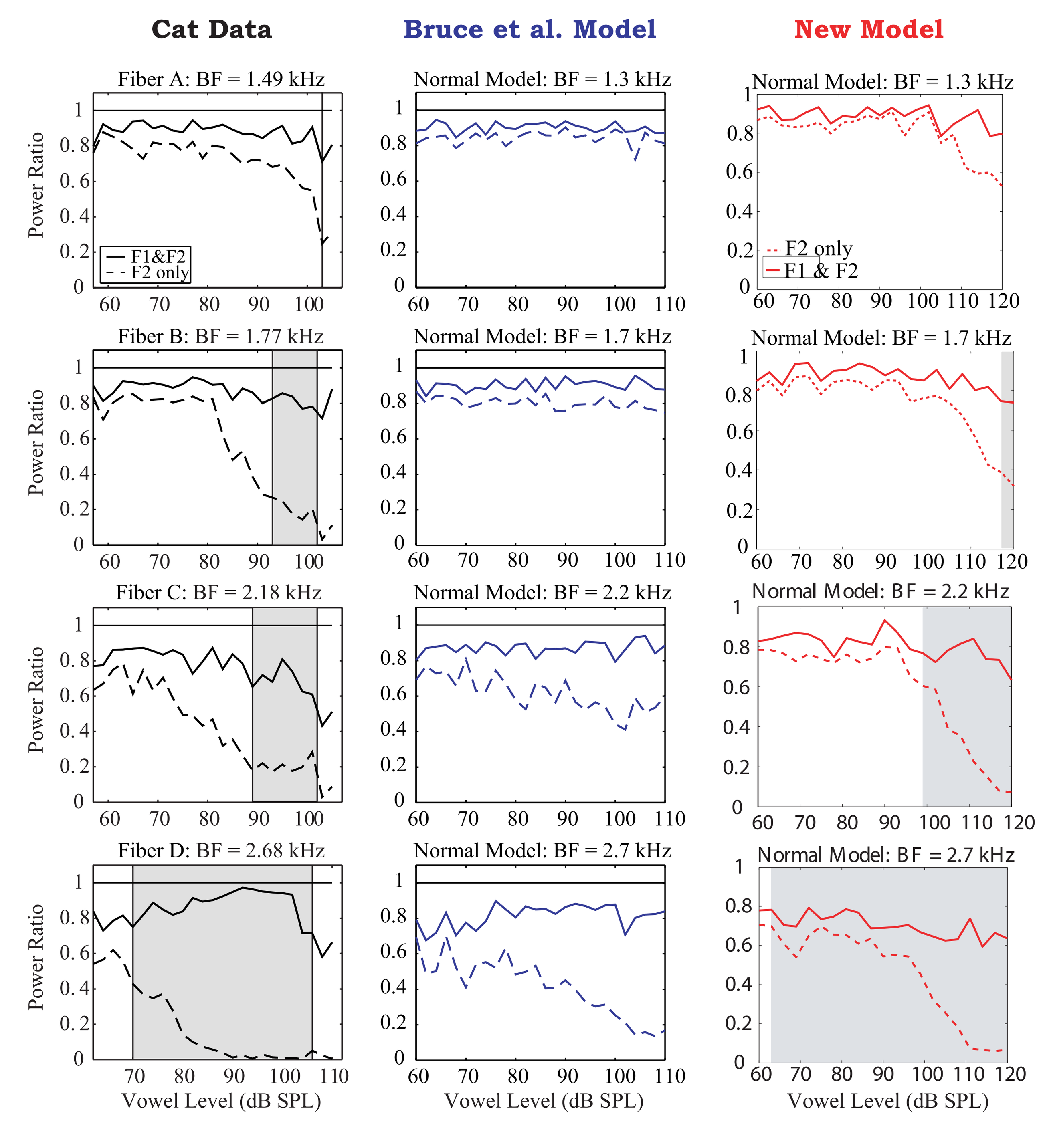

Fig. 7. Normal power ratio (PR) data at high sound levels for four normal fibers with BFs as labeled. The solid and dashed lines, respectively, show the fraction of total power in the fiber's response that is synchronized to F1 and F2 combined (F1 & F2) or to F2 alone. Total power is the sum of the squares of the synchronized rates over the first 20 harmonics of the stimulus. F1 & F2 related power is the sum of the squares of the synchronized rates at the harmonics related to F1 and F2, which include the 5th, 7th, 10th, 12th,15th, 17th and 20th harmonics. The F2 PR is the fraction of the total power that is phase-locked to the second formant (17th harmonic). The F1 & F2-related PR is the fraction of the total power contained in the f1 & F2-related harmonics. The lower and upper bounds of the shaded regions represents, respectively, the sound levels at which a loss of synchrony capture by F2 occurs and the component 2 threshold for F1. Left column: Redrawn from Fig.4 of Wong et al. (1988). Middle column: Results from Bruce et al. (2003). Right column: Results from the new model.

4. Discussions and Conclusions

This poster describes a computational model that is accurate enough to be useful in testing the effects of potential hearing aid processing schemes on the neural representation of speech. The added feature of level-independent frequency glides in the impulse response of AN fibers into the Bruce et al. model gives more realistic AN responses for the vowel stimuli. The realization of BF shift in the impaired cochlea or at high intensities in the normal cochlea in this model helps to describe the loss of synchrony from the second formant to the first at high intensities or in the impaired cochlea. However, the impaired model still shows overestimated synchrony to F2 in the BF region around F2. Also, only AN fibers with high spontaneous rates have been cosidered here.

The parameters of the Boltzmann function in the control path shows a significant effect on the behaviour of compression which is partly responsible for the loss of synchrony from F2 to F1 at high intensities. We are still working on this new model to be able to more accurately predict the amount of synchrony loss by F2 in the normal and impaired cases. For this, we need to adjust the parameters of the Boltzmann function and also the BM chirp filter.

One important feature that is not addressed is the component 1/component 2 transition. A change in AN responses occurs at high levels that is characterized by an abrupt shift of 180° in the phase of the response over a few dB. Usually C2 responses are poorly tuned. In acoustically traumatized cats, C1 responses are significantly attenuated while C2 responses are robust and resistant to trauma. These additions to the model should further improve its accuracy and utility as a means of developing and testing potential hearing-aid speech processing schemes for sensorineural hearing loss.

References

[1] Bruce IC, Sachs MB, Young ED. An auditory-periphery model of the effects of acoustic trauma on auditory nerve responses. J. Acoust. Soc. Am. 113: 396–388, 2003.

[2] Tan Q, Carney LH. A phenomenological model for the responses of auditory-nerve fibers. II. Nonlinear tuning with a frequency glide. J. Acoust. Soc. Am. 114: 2007-2020, 2003.

[3] Carney LH. A model for the responses of low-frequency auditory-nerve fibers in cat. J. Acoust. Soc. Am. 93: 401-417, 1993.

[4] Zhang X, Heinz MG, Bruce IC, Carney LH. A phenomenological model for the responses of auditory-nerve fibers: I. Nonlinear tuning with compression and suppression. J. Acoust. Soc. Am. 109: 648–670, 2001.

[5] Carney LH, McDuffy MJ, Shekhter I. Frequency glides in the impulse responses of auditory-nerve fibers. J. Acoust. Soc. Am. 105: 2384-2391, 1999.

[6] Wong JC, Miller RL, Calhoun BM, Sachs MB, Young ED. Effects of high sound levels on responses to the vowel /e/ in cat auditory nerve. Hearing Research. 123: 61-77, 1998.

[7] Miller RL, Schilling JR, Franck KR, Young ED. Effects of acoustic trauma on the representation of the vowel /ε/ in cat auditory-nerve fibers. J. Acoust. Soc. Am. 101(6):3602–3616, 1997.

[8] Heijden MVD, Joris PX. Cochlear phase and amplitude retrieved from the auditory-nerve at arbitrary frequencies. The Journal of Neuroscience, 23 (27): 9194-9198, 2003.

[This work was supported by NSERC Discovery Grant 261736 and the Barber-Gennum Chair Endowment.]